processes

MDPI

Article

Research on Well Pattern Optimization Method for Multilayer Thin Gas Reservoir Based on DNN Algorithm

Liang Liang [1,2], Youyou Cheng [1,2], Xiang Luo [1,2], Linhao Qiu [1,2] and Chengqian Tan [1,2,*]

[1] School of Earth Sciences and Engineering, Xi'an Shiyou University, Xi'an 710065, China; lyj200009232517@163.com (L.L.); wd29871101@163.com (Y.C.); luoxiangxsyu@163.com (X.L.); qlh6927@163.com (L.Q.)
[2] Shaanxi Key Laboratory of Petroleum Accumulation Geology, Xi'an Shiyou University, Xi'an 710065, China
* Correspondence: daidaoxiaowei33@163.com; Tel.: +86-187-0911-2987

Abstract: Conventional development technologies for gas reservoirs have made significant advancements, particularly in well pattern optimization, enhanced recovery, and dynamic monitoring. However, multilayer thin gas reservoirs face challenges such as strong heterogeneity, thin effective thickness, poor interlayer connectivity, and difficulties in characterizing dynamic features. These factors complicate the direct application of traditional well pattern optimization methods. The gas reservoir in the western part of Block B, Right Bank of the Amu River, serves as a typical example of a multilayered thin gas reservoir. This study aims to optimize well patterns for composite layer development. A numerical simulation model is established and verified through historical fitting of production data. Using the DNN algorithm and 150 orthogonal experimental models, the optimal horizontal well pattern is determined, with a training error of 7.6% when the training set reached 120 sets. Five optimization charts for multilayer thin gas reservoirs are developed, improving the reservoir recovery factor and supporting efficient production. This work provides a theoretical foundation for the development of similar multilayer composite gas reservoirs.

Keywords: Deep Neural Network (DNN); multilayer thin gas reservoir; numerical simulation; well pattern optimization

check for updates

Academic Editor: Qingbang Meng

Received: 10 January 2025
Revised: 12 February 2025
Accepted: 16 February 2025
Published: 20 February 2025

Citation: Liang, L.; Cheng, Y.; Luo, X.; Qiu, L.; Tan, C. Research on Well Pattern Optimization Method for Multilayer Thin Gas Reservoir Based on DNN Algorithm. *Processes* **2025**, *13*, 599. https://doi.org/10.3390/pr13030599

Copyright: © 2025 by the authors. Licensee MDPI, Basel, Switzerland. This article is an open access article distributed under the terms and conditions of the Creative Commons Attribution (CC BY) license (https://creativecommons.org/licenses/by/4.0/).

1. Introduction

With the continuous growth in global natural gas demand, the development of gas reservoirs faces increasing challenges. While conventional gas reservoir development has become relatively mature from a technical perspective, the issues of economic viability and sustainability have become more prominent as resources gradually deplete [1–3]. Consequently, more research has focused on how to optimize development plans to enhance recovery factors and economic benefits. Among these optimization strategies, well pattern optimization has garnered widespread attention as one of the core technologies for improving recovery rates and reducing development costs [3]. At the same time, the development of multilayer thin gas reservoirs has become a new focus in the oil and gas industry. Their unique geological characteristics make well pattern optimization even more complex [4]. This paper begins with a review of research progress in conventional gas reservoir well pattern optimization and gradually transitions to the development strategy and well pattern optimization research for multilayer thin gas reservoirs, analyzing their significance in modern oil and gas exploration.

Well pattern optimization in conventional gas reservoirs primarily focuses on improving well connectivity and gas recovery. Over the past few decades, numerous achievements have been made in the optimization of well patterns for conventional gas reservoirs. Early studies concentrated on optimizing gas reservoir development by adjusting well placement and spacing [2,5–7]. For instance, He D.B., Jia A.L., Ji G., et al. proposed a well pattern optimization design based on reservoir characteristics and development needs, which effectively improved the recovery factor of conventional gas reservoirs [8,9]. With the development of numerical simulation technology, researchers have adopted more refined fluid flow models to optimize well placement and enhance development efficiency. Liu J., Liu Y.T., Zhang J.C., et al. integrated numerical simulation with reservoir pressure data and proposed an improved well pattern optimization method, which provides customized well layouts for different stages of development to suit the characteristics of various reservoirs [10]. Jang I., OH S., Kim Y., et al. further introduced artificial intelligence algorithms and used big data analysis techniques to optimize well placement, thereby enhancing the development efficiency and economic benefits of conventional gas reservoirs [11]. Mousavi and Hosseini-Nasab proposed several innovative methods that significantly improve the lithological classification accuracy of oil and gas reservoir formations. Mousavi et al. introduced a novel approach based on deep learning for rapid and accurate prediction of lithology in oil and gas fields. This method involves converting conventional wellbore data into two-dimensional images and efficiently training them with a residual convolutional neural network (ResCNN). The method demonstrated excellent performance across multiple datasets, particularly in terms of data balancing, which enhanced the model's accuracy and F1-score. Hosseini-Nasab et al., on the other hand, applied advanced machine learning and deep learning techniques, proposing three new algorithms, including GrowNet, Deep-Insight, and Blender. These algorithms address data imbalance issues and significantly improve lithological classification performance. In particular, Deep-Insight converts tabular data into image inputs for convolutional neural networks, greatly enhancing classification accuracy and showcasing the immense potential of deep learning technologies in complex reservoir geological evaluations [12,13].

Multilayer thin gas reservoirs refer to gas reservoirs with thin layers and complex stratigraphy. Compared with conventional gas reservoirs, these reservoirs are typically more challenging to develop, but their potential resource value and strategic significance are gradually being recognized. As conventional gas reservoirs are progressively depleted, the development of deeper and tighter gas reservoirs has become an inevitable trend for the global oil and gas industry. Multilayer thin gas reservoirs often contain rich natural gas resources, and their development value is increasingly realized through technological innovation and optimization of extraction methods [14]. The development of these reservoirs not only provides strong support for energy supply, but also effectively promotes regional economic development, drives energy structural transformation, and reduces dependence on traditional fossil fuels. In China's Sichuan Basin and the U.S. Piceance Basin, the high-efficiency development of multilayer thin gas reservoirs has been achieved through the use of advanced horizontal drilling and fracturing technologies [15]. Therefore, the development of multilayer thin gas reservoirs is of great strategic significance and will play a key role in future energy supply.

As the development of multilayer thin gas reservoirs advances, well pattern optimization has become a key technology for improving development efficiency and recovery rates. Compared to conventional gas reservoirs, the well pattern optimization for multilayer thin gas reservoirs faces greater challenges, mainly due to the complexity of the reservoir and differences in interlayer connectivity. Multilayer thin gas reservoirs exhibit strong geological heterogeneity, with thin and complex layers. Therefore, a single well pattern

optimization strategy cannot meet the development needs [16]. Hu W.R., Wei Y., and Bao J.W. proposed a well pattern optimization method based on layered development, emphasizing the use of different well placement and fracturing techniques for different layers to improve connectivity between layers. Wei S.M. and Qiu K.X. used geological modeling and fluid simulation to propose a well pattern optimization scheme based on interlayer pressure gradients, which adjusts well layouts according to the reservoir's characteristics, thereby improving overall recovery rates [4].

Additionally, with the continuous development of gas injection and fracturing technologies, more studies have begun integrating these techniques with well pattern optimization. Qun L., Yun X., BO C., et al. proposed a novel well pattern optimization method for multilayer thin gas reservoirs by combining big data with artificial intelligence [8,17]. This method uses high-precision geological modeling and fluid flow simulation to design optimization plans that improve the development efficiency of multilayer gas reservoirs. Feng X.X. and Liao X.W. analyzed the layout of gas injection and fracturing wells and proposed a comprehensive well pattern optimization strategy, emphasizing precise interlayer management and optimization of gas injection technologies to enhance the development of multilayer thin gas reservoirs. These research results suggest that well pattern optimization for multilayer thin gas reservoirs requires consideration of not only reservoir and fluid characteristics, but also the integration of advanced gas injection and fracturing technologies for efficient development [18–21].

Although these studies provide theoretical foundations and technical support for well pattern optimization in carbonate gas reservoirs, systematic research on the complex conditions of multiple gas–water systems and thin and heterogeneous reservoirs is still insufficient. There is a lack of refined evaluation and optimization methods. This study employs 3D geological modeling and numerical simulation techniques to extract eight typical parameters and design 150 orthogonal experimental models. The orthogonal experimental model is a method that systematically arranges experimental conditions and combinations to obtain the optimal solution with the fewest experimental runs, commonly used in engineering optimization research. By integrating the Deep Neural Network (DNN) model, a typical well pattern parameter selection chart for the study area is constructed. The numerical simulation results for the study area show a single well fitting rate of over 90.2%, with a net present value (NPV) error of 7.6% for single wells using the DNN model and a horizontal section length error of 7.85%. These results indicate high accuracy and can guide practical production activities.

2. Geological Background

The Amu Darya Right Bank Gas Field is located in the Amu Darya Basin (as shown in Figure 1), a large Mesozoic superimposed sedimentary basin in the southeastern part of the Turan Platform. The basin's basement is composed of Paleozoic igneous and metamorphic rocks. Above the basement, a sequence of layers is developed, including the Permian–Triassic terrestrial clastic transition layer, the coal-bearing sand and mudstone of the Middle and Lower Jurassic coastal plain-shallow marine facies, the marine carbonate rocks and evaporites of the Upper Jurassic, and the carbonate rocks, evaporites, and sand-mudstone of the Cretaceous–Paleogene. The basin's tectonic structure and sedimentary cover distribution are mainly controlled by two sets of faults trending northwest and northeast [1].

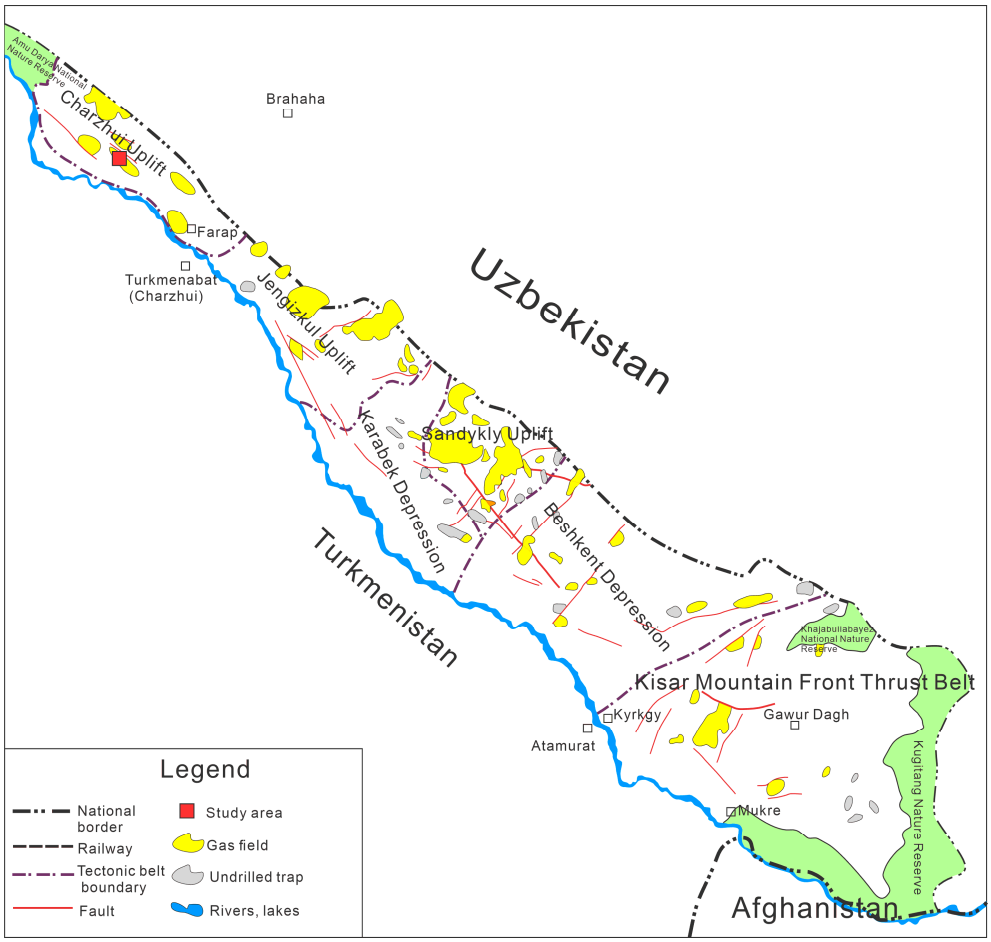


Figure 1. Geographical and regional structural location map of the study area.

The reservoir in the Amu Darya Right Bank Gas Field primarily consists of Upper Jurassic Kharif–Oxfordian marine carbonates, dated around 164.7–155.7 million years ago. As shown in Figure 2. The primary hydrocarbon source rock for the gas field is the coal-bearing sequence from the Middle to Lower Jurassic, with the cap rock being a gypsum salt layer from the Upper Jurassic Basma-Li stage. The gas field's reservoirs exhibit two main structural types: dome-shaped large anticlines and overthrust structures. The large anticline structure is located in the western part of the gas field and is characterized by a large scale with a relatively short axis, forming a broad, gentle fold. The overthrust structure, located in the eastern part of the gas field, developed in the background of the basement fault block uplift and is smaller in scale, representing a local structure. The carbonate gas reservoirs in these two structural types differ significantly in terms of burial depth and stratigraphic sequence.

Compared to the large anticline structure, the carbonate gas reservoirs in the overthrust structure are buried deeper and lack the upper carbonate layers found in the large anticline structure. The carbonate sedimentary facies in the large anticline structure are diverse, including platform-edge bio-reefs, reef limestones from shallow beach facies, bio-clastic limestones, and oolitic limestones, with relatively high dolomitization content. In contrast, the carbonate reservoirs in the overthrust structure are mainly composed of mudstone, fine-grained limestone, and particle limestone from the platform-front gentle slope facies, with lower dolomitization content [22].

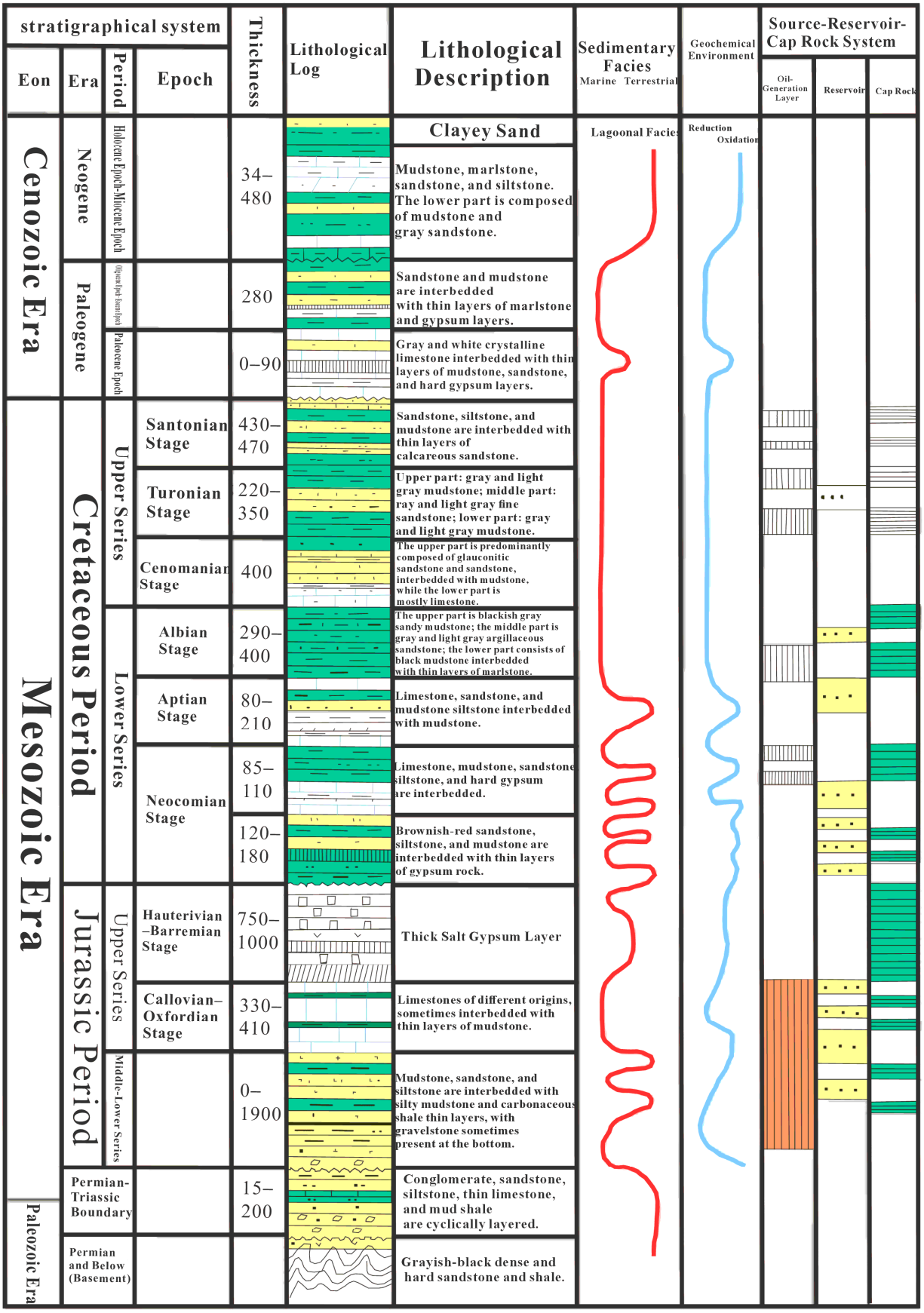


Figure 2. Stratigraphic sequence characteristics of the study area.

2.1. Establishment of Geological Models and Numerical Models

Based on the single well data, seismic data, geophysical research results, and geological foundation research results of the study area, geological modeling of the gas reservoir was conducted using Petrel (2018) software. The numerical simulation model was built using tNavigator software (2020.2 Version.), considering the reservoir and fluid properties, as well as the development conditions of the study area. According to the reservoir analysis results from well logging, the vertical grid size of the main productive layers in the geological modeling was set to 0.5–1 m. The working area covers approximately 480 km^2 with sparse well distribution (the minimum well spacing is about 3000 m), and the well positions are scattered. The horizontal grid was designed as 50 m by 50 m. The geological grid consists of 85,075,680 cells (744 × 363 ×315), with XVac: 90 layers, XVp: 25 layers, XVm: 60 layers, and XVa1: 60 layers.

A fault model is established using the fault data interpreted from seismic data. Based on the interpreted seismic layers and combined with the geological stratification data of each small layer, a stratigraphic and structural framework model is built [23]. The model results of the study area are shown in Figure 3 below. (Among them, XVac, XVp, XVm, XVhp, XVa1, XVz, XVa2, and XVI are the main target layers of the study area, belonging to the Kallov–Oxford stage.)

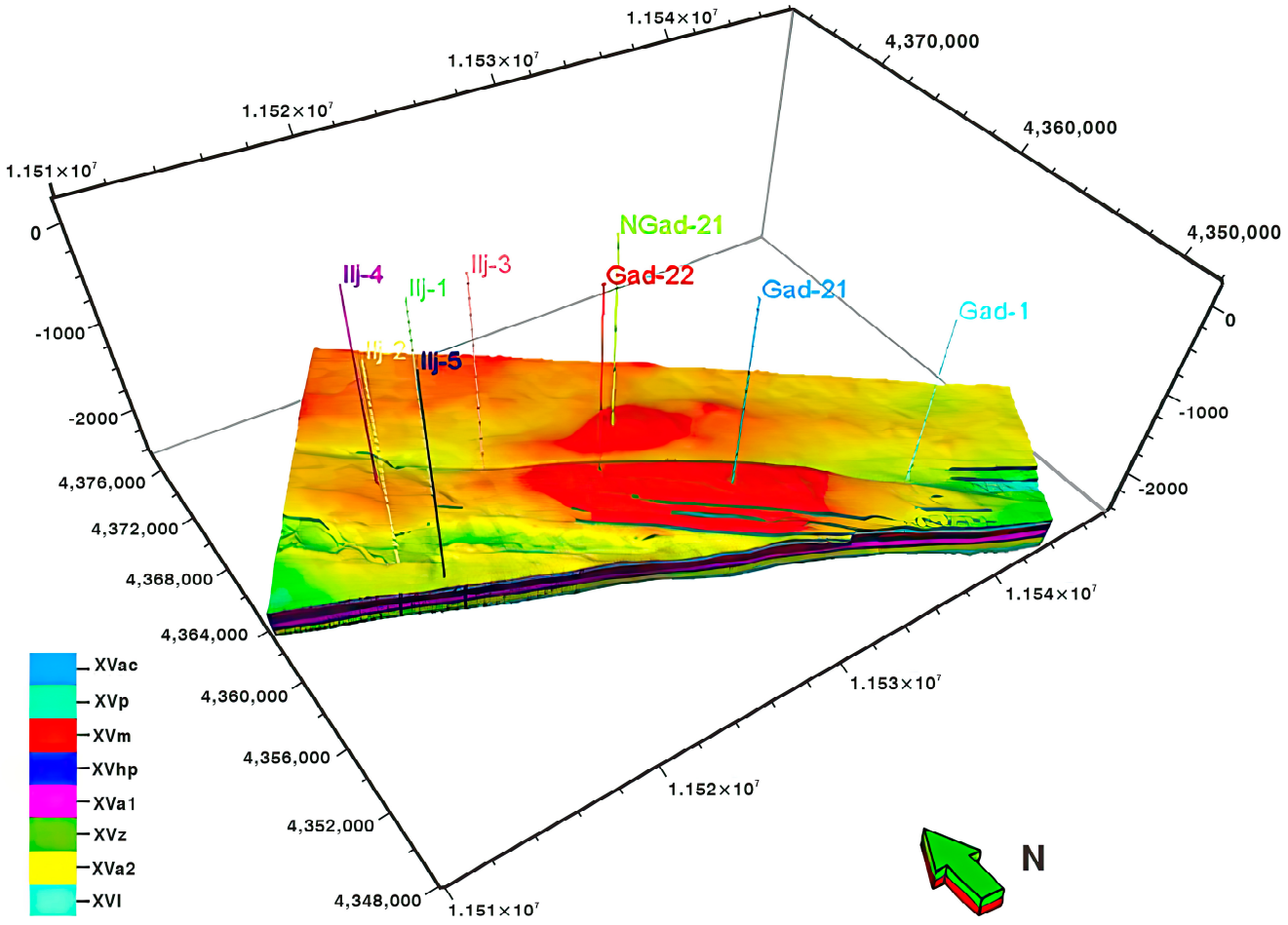


Figure 3. Stratigraphic and structural model of the study area.

Using the results of seismic impedance inversion as constraints, the sequential Gaussian simulation method is applied to establish the three-dimensional spatial distribution of reservoir properties. The basic parameters of the model for the study area are shown in Table 1. The reservoir property model for the study area, established based on the

parameters in Table 1, is shown in Figure 4, which includes (a) the porosity model, (b) the permeability model, and (c) the water saturation model.

Table 1. Basic Parameters of the model (where G and N-G represent gas wells in the study area, respectively).

Parameter		Value	Remarks
Model	Grid	Plane: Corner-point grid; Vertical: 29 layers	
	Single well production (10^3 m^3/d)	255	
Reservoir Properties	Reservoir thickness (m)	115	Porosity, permeability, and thickness values assigned as averages for each small layer, values derived from the geological model
	Average porosity (%)	10.43	
	Average permeability (mD)	3.94	
Water Body Multiplier	G	2.0	XVac, XVp, XVm are the primary development layers
	N-G	7.0	
Reserves (10^9 m^3)	G	17.0	
	N-G	7.1	

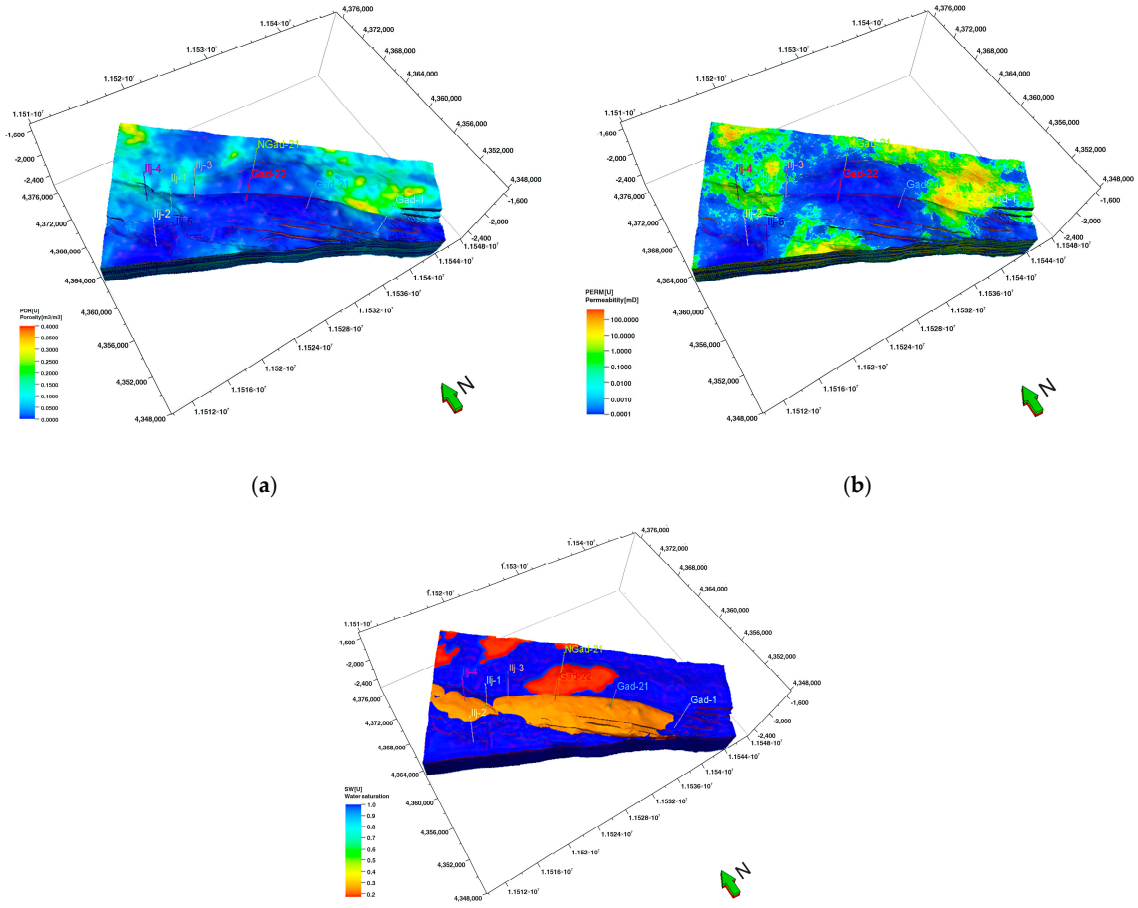


Figure 4. Reservoir property model of the study area; (**a**) porosity model; (**b**) permeability model; (**c**) water saturation model.

To assess the reliability of the geological model, this study combines the reservoir geological model with the volumetric method for a comparative analysis of the reserves. A detailed comparison was made between the reserves calculated using the geological model and those calculated using the volumetric method. The results showed that both methods yielded very similar outcomes. Specifically, the difference between the reserves estimated by the geological model and those estimated by the volumetric method is small, with both absolute and relative errors remaining within a very low range. Based on these results, it can be concluded that the reserve estimates from both the geological model and the volumetric method are highly consistent, indicating that the constructed geological model has a high level of accuracy and reliability in reserve estimation. This suggests that the model effectively reflects the actual conditions of the gas reservoir, providing a solid foundation for subsequent development decisions [2,24–26].

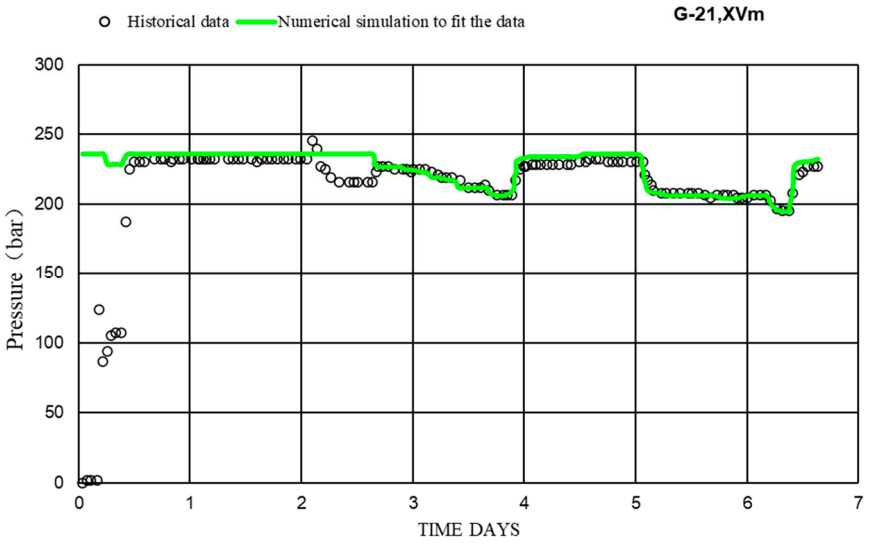
A numerical simulation model of the gas reservoir was established based on the geological model of the study area, and a history matching study was carried out. The specific fitting results are shown in Figure 5 below. As can be seen from the figure, the fitting results show a high degree of agreement with the historical data. Through calculations, we have determined that the single well fitting rate in the study area exceeds 90.2%.

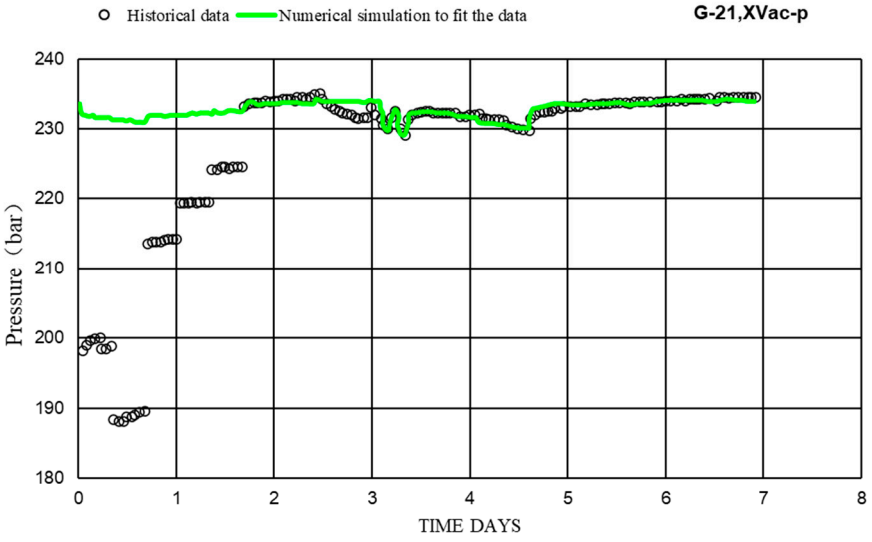
2.2. Well Pattern Optimization

In conventional gas reservoir well pattern optimization studies, the selected parameters mainly include well spacing, well type (e.g., vertical wells, horizontal wells), fracturing schemes, gas production rates, etc. The selection and optimization of these parameters mainly focus on key factors such as reservoir permeability, thickness, pressure gradient, and gas production. The core objective of conventional gas reservoir well pattern optimization is to improve the inter-well connectivity of the reservoir through reasonable well layout, optimize development costs and recovery rates, and, in turn, enhance economic efficiency [17,27–30].

In the well pattern optimization study of multilayer thin gas reservoirs, due to the high heterogeneity of the reservoir structure, complex layering, and large variations in reservoir thickness, the optimization parameters are more complex than those in conventional gas reservoirs. Therefore, when conducting well pattern optimization for multilayer thin gas reservoirs, in addition to considering factors such as reservoir permeability, pressure gradient, and well pattern layout, it is also necessary to take into account interlayer connectivity, pressure differences between layers, gas production from each layer, and the presence of interlayer water barriers. A comprehensive selection of parameters, such as well location, well spacing, staged fracturing technology, and gas injection schemes, should be carried out to perform targeted well pattern optimization research [31–36].

Due to the limited number of wells in the study area, the wells in this study are arranged in a radial pattern to optimize reservoir drainage. The spacing between the wells is determined based on the reservoir's heterogeneity and production characteristics, with a focus on ensuring effective contact with the main production zones of the reservoir. The wells are primarily located at the center and the highest production areas of the reservoir to maximize recovery rates, while minimizing interference between the wells.





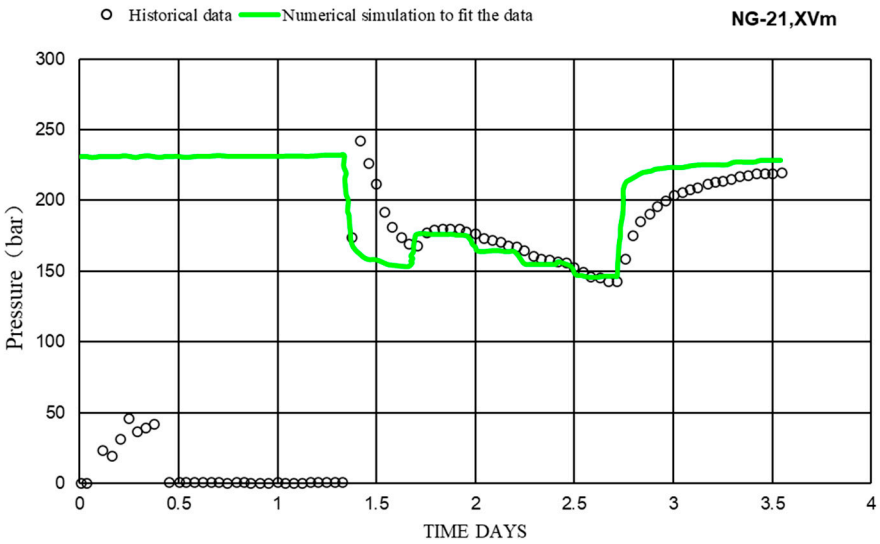


Figure 5. *Cont.*

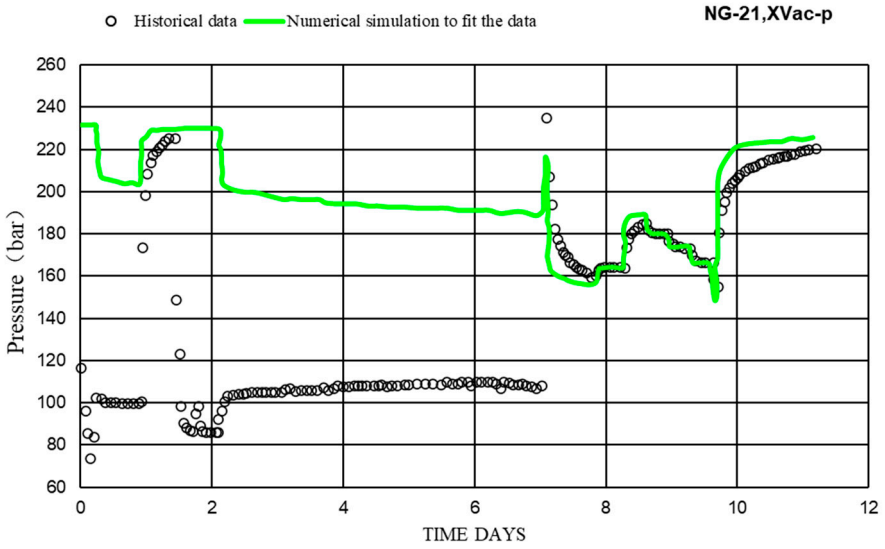


Figure 5. History matching diagram of the gas reservoir in the study area.

In the development of multilayer thin gas reservoirs, the unit length drainage degree is one of the key parameters for evaluating development effectiveness. The unit length drainage degree is mainly evaluated by considering the amount of gas reservoir resources developed per unit length and the input-output ratio of wells. This indicator can effectively reflect the rationality of well placement and the impact of well distribution on factors such as reservoir permeability and gas production. For the multilayer thin gas reservoirs in the study area, excessive well spacing or improper well type selection may lead to uneven reservoir development, thereby reducing the overall recovery rate of the gas reservoir. Therefore, by optimizing the unit length drainage degree, the best resource recovery effect can be achieved within the limited development area, improving the economic efficiency of the development.

As shown in Figure 6, by calculating the unit length drainage degree for different well types, it was found that vertical wells had a higher unit length drainage degree, while stepped horizontal wells had the longest stable production period.

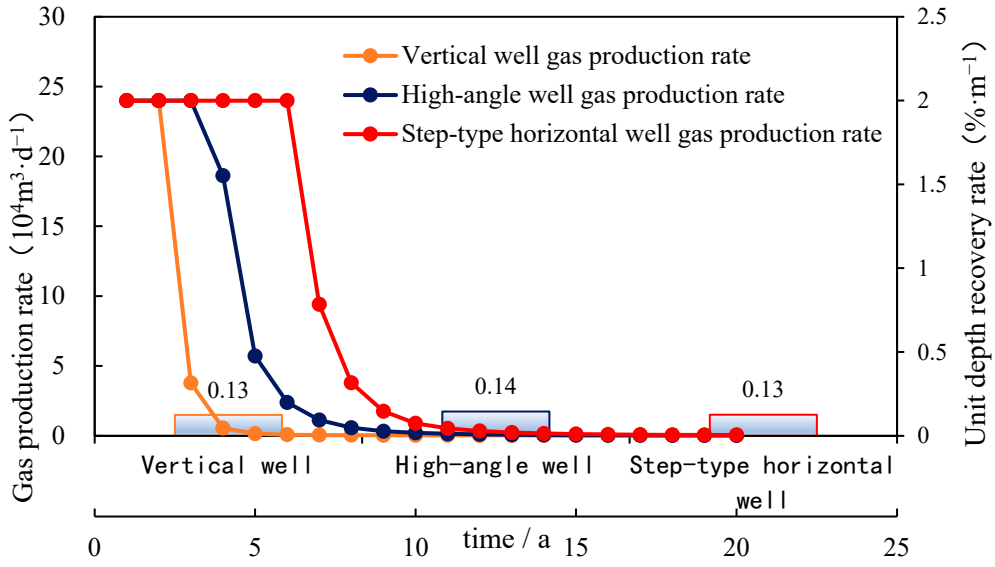


Figure 6. Unit length drainage degree and gas production rate variation curves for different well types.

On the other hand, the single well financial net present value (FNPV) model focuses on evaluating the development potential of well types from an economic perspective. This model compares the revenue of a single well with its development costs, taking into account all financial factors, including natural gas prices, equipment investment, operating costs, taxes, etc., to help determine the economic viability of the well.

The calculation formula is as follows:

$$FNPV = \sum_{t=0}^{n} \frac{CF_t}{(1+r)^t} - I_0 \quad (1)$$

In the formula, CF_t represents the cash flow in year t, including sales revenue, operating costs, and taxes; r is the discount rate, which refers to the capital cost or expected return rate of the project; t represents the year, where $t = 0$ indicates the year of initial investment, and $t = 1, 2, \ldots, n$ represents the future annual cash flows; n is the total project lifespan, which in this case refers to the expected production life of the gas well; I_0 is the initial investment, which includes the drilling cost of the gas well and other related investments.

By calculating and analyzing the financial net present value (FNPV) of different well types in the multilayer thin gas reservoirs of the study area, the profitability of different well types over the long term can be quantified. The application of the NPV model indicates that selecting the appropriate well type can not only effectively reduce development costs but also increase the overall return rate of the gas reservoir. The analysis results using the single well FNPV model for the study area, as shown in Figure 7, demonstrate that stepped horizontal wells perform better economically compared to traditional vertical wells and conventional horizontal wells.

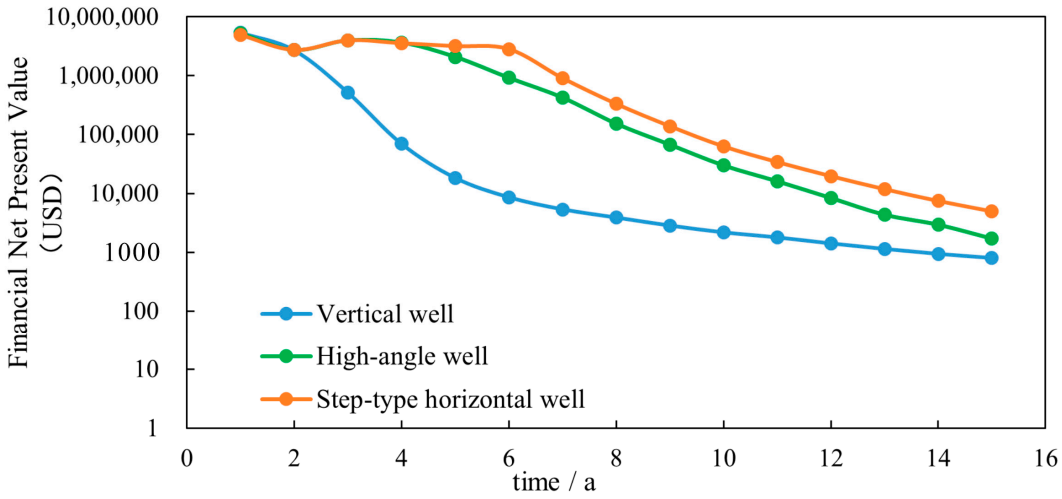


Figure 7. Variation curves of financial net present value for different well types over 15 years of production.

Through the comparative analysis using the unit length drainage degree and single well financial net present value (NPV) model, the stepped horizontal well is selected as the optimal development well type for the multilayer thin gas reservoirs in the study area. This well type can effectively improve well-to-well connectivity, cover multiple thin reservoir layers, and optimize the gas reservoir development efficiency and economic benefits. It has a higher resource recovery rate and lower development costs compared to traditional well types, making it the most suitable for gas reservoir development in this region.

Since there are many factors affecting the well network capacity of stepped horizontal wells, the main orthogonal factors considered in this study include well spacing, well number, horizontal section proportion, and well network direction. Each factor has four

levels (Table 2). The optimization goal is to maximize the net present value of the horizontal well while ensuring practical applicability. The experimental design and corresponding numerical calculation results are shown in Table 2.

Table 2. Factor levels for well network optimization.

Level	Factors			
	Well Spacing/m	Well Number/Count	Horizontal Section Proportion	Well Network Direction/°
1	1500	8	1:1:2	N-W 80
2	2000	6	1:1:1	N-W 20
3	2500	5	1:1:1	N-W 80
4	3000	3	1:1:2	N-W 20

(**Horizontal Section Proportion** refers to the ratio of the length of a specific horizontal section of the wellbore to the total length of the horizontal section within a given well pattern. This proportion is used to assess the distribution and effectiveness of the horizontal wellbore in different sections of the reservoir, helping to optimize the well placement and enhance reservoir management strategies.)

Based on a 4-parameter, 4-level orthogonal experimental design, 16 experimental groups were established to optimize the well network parameters for the stepped horizontal wells in the study area. The objective of the experiment was to achieve the highest possible net present value (NPV) of the horizontal wells while maximizing the predicted ultimate recovery, balancing both factors to determine the optimal combination of structural parameters. The orthogonal experimental design and simulation results are presented in Table 3.

Table 3. Orthogonal experimental design and simulation results.

Experiment No.	Factors				Horizontal Segment Length/m	Steady-State Production Period/a	Predicted Recovery Factor at the End of the Forecast Period/%	Net Present Value/$10^9$$
	Well Spacing/m	Well Number/Count	Horizontal Segment Ratio	Well Network Direction/°				
1	1500	8	1:1:2	N-W 80	700	12	78.35	2.611
2	2000	6	1:1:1	N-W 20	500	10	73.18	2.675
3	2500	5	1:1:1	N-W 80	900	7	70.64	2.706
4	3000	3	1:1:2	N-W 20	300	2	54.75	1.927
5	1500	8	2:1:1	N-W 20	900	12	78.93	2.590
6	2000	6	1:2:1	N-W 80	300	10	72.64	2.631
7	2500	5	1:2:1	N-W 20	700	7	69.21	2.729
8	3000	3	2:1:1	N-W 80	500	2	55.96	2.094
9	1500	8	1:2:1	N-W 120	500	13	77.41	2.642
10	2000	6	2:1:1	N-W 40	700	10	73.76	2.661
11	2500	5	2:1:1	N-W 120	300	8	63.08	2.676
12	3000	3	1:2:1	N-W 40	900	1	58.82	2.234
13	1500	8	1:1:1	N-W 40	300	13	76.32	2.639
14	2000	6	1:1:2	N-W 120	900	9	74.21	2.631
15	2500	5	1:1:2	N-W 40	500	8	67.92	2.741
16	3000	3	1:1:1	N-W 120	700	2	57.24	2.087

(**Horizontal Segment Ratio** refers to the ratio of the number of horizontal well segments within a specific section of the wellbore to the total number of well segments in the entire well pattern. This ratio is used to evaluate the segmentation and distribution of horizontal well segments across the reservoir, providing insights into the optimization of wellbore design for maximizing reservoir contact and enhancing production efficiency.)

For the indicator of net present value (NPV), when the well spacing is 1500 m, the average NPV is 2.620 $\times$ $10^9$$; when the well spacing is 2000 m, the average NPV is 2.650 $\times$ $10^9$$; when

the well spacing is 2500 m, the average NPV is 2.713 × 10^9\$; and when the well spacing is 3000 m, the average NPV is 2.086 × 10^9\$. Therefore, the maximum NPV is achieved when the well spacing is 2500 m. Similarly, the maximum NPV of 2.713 × 10^9\$ is obtained when the number of wells is 5. The optimal horizontal segment ratio is 1:2:1, which results in the maximum NPV of 2.559 × 10^9\$, and the maximum NPV of 2.577 × 10^9\$ is achieved when the well network orientation is N-W-40°.

Based on the priority order of these influencing factors, the next step is to calculate the result values corresponding to each level of each factor. The calculated results for each factor and its corresponding level of NPV are summarized in Table 4, where K_{jm} represents the optimization index corresponding to the mth level of the jth factor.

Table 4. Statistical data of range analysis for orthogonal experiment (net present value).

K_{jm} of Each Level	Net Present Value/10^9\$			
	Well Spacing/m	Well Number/Count	Horizontal Segment Ratio	Well Network Direction/°
1	2.713	2.713	2.559	2.569
2	2.650	2.650	2.527	2.510
3	2.620	2.620	2.505	2.509
4	2.086	2.086	2.478	2.480

Through the data analysis in Table 4, the optimal factor level combination is selected as follows: well spacing of 2500 m, number of wells 5, horizontal section ratio of 1:2:1, and well network direction of N-W 40°.

Using the same method for the net present value indicator, the range of each factor for the predicted cumulative recovery degree at the end of the forecast period is calculated as follows:

Through the data analysis in Table 5, the optimal factor-level combination was selected as follows: well spacing of 2500 m, 8 wells, horizontal segment ratio of 1:2:1, and well network direction N-W80°. Based on the requirements of this experiment, the final optimized factor-level combination was determined as well spacing of 2500 m, 5 wells, horizontal segment ratio of 1:2:1, and well network direction N-W80°.

Table 5. Orthogonal experiment range analysis data statistics (predicted cumulative recovery degree at the end of forecast period).

K_{jm} of Each Level	Predicted Recovery Factor at the End of the Forecast Period/%			
	Well Spacing/m	Well Number/Count	Horizontal Segment Ratio	Well Network Direction/°
1	77.7525	77.7525	68.8075	69.3975
2	73.4475	73.4475	69.345	69.0175
3	67.7125	67.7125	67.9325	67.985
4	56.6925	56.6925	69.52	69.205

Numerical simulation methods are essentially enumeration methods. For a given reservoir, a large number of scenarios are needed to complete the well network verification. When the reservoir conditions are unknown, the primary influencing factors of the well network parameters are designed into 3 categories with a total of 18 variations. Relying solely on conventional orthogonal experiments, it is almost impossible to achieve global optimization of well network parameters. Therefore, to perform a well network parameter verification under different reservoir conditions, 8 representative typical parameters were selected, and a multi-parameter orthogonal experimental scheme with 150 sets was designed, as shown in Table 6. This approach was used to conduct detailed numerical simulation studies, providing basic samples for subsequent well network optimization.

Table 6. Multilayered reservoir well network optimization orthogonal experimental design table.

Type	Parameter	Permeability/10^{-3} μm²		Effective Gas Layer Thickness/m	Gas Layer Thickness Ratio	Water Multiplication Factor	Interlayer Initial Pressure Difference/MPa	Gas Viscosity Ratio per Layer	Horizontal Section Length/m	Horizontal Section Ratio	Well Spacing/m	Number of Wells/Count	Well Network Orientation/°
		K_{max}	K_{min}										
Reservoir Characteristics Parameters	Permeability Gradient	0.5	0.5	20	1:1:2	3	1	1:2:1	300	1:2:1	1500	18	N-W 20
		1.0							500	1:1:2	2000	14	N-W 40
		2.5							700	1:3:1	2500	11	N-W 80
		5.0							900	1:1:3	3000	8	N-W 120
	Gas Layer Thickness Ratio	0.5		10	1:1:2 1:1:3 1:2:1 2:1:1	3	1	1:2:1	300	1:2:1	1500	18	N-E 20
				30					500	1:1:2	2000	14	N-E 40
				30					700	1:3:1	2500	11	N-E 80
				40					900	1:1:3	3000	8	N-E 120
	Interlayer Initial Pressure Difference/MPa	0.5		20	1:1:2	3	1	1:2:1	300	1:2:1	1500	18	N-W 20
							2		500	1:1:2	2000	14	N-W 40
							3		700	1:3:1	2500	11	N-W 80
							4		900	1:1:3	3000	8	N-W 120
Fluid and Other Parameters	Water Multiplication Factor	0.5		20	1:1:2	1	1	1:2:1	300	1:2:1	1500	18	N-E 20
						3			500	1:1:2	2000	14	N-E 40
						6			700	1:3:1	2500	11	N-E 80
						9			900	1:1:3	3000	8	N-E 120
						12							
	Gas Viscosity Ratio per Layer	0.5		20	1:1:2	3	1	1:1:2 1:2:1 2:1:1 1:1:3	300	1:2:1	1500	18	N-E 20
									500	1:1:2	2000	14	N-E 40
									700	1:3:1	2500	11	N-E 80
									900	1:1:3	3000	8	N-E 120

3. Neural Network Prediction Methods

In this study, orthogonal experimental design was initially employed to explore the impact of multiple factors on the target variables. However, due to the need to compute a large number of combinations of factors and levels in orthogonal experiments, the computational workload became excessive, significantly reducing the overall work efficiency. The complexity of data processing and the time-consuming manual calculations made it difficult to scale this experimental design effectively. To address this issue, we introduced the Deep Neural Network (DNN) algorithm, which is capable of learning complex patterns and relationships from large-scale datasets [13,28,37–40]. The DNN not only improved computational efficiency by automating the data analysis process but also enhanced predictive accuracy by modeling the nonlinear interactions between factors [12]. Simulation results from numerical modeling methods were used as input, with 80% of the data selected for training and the remaining 20% used to test the accuracy of the predictions. This approach ultimately optimized well network parameters for multilayered gas reservoirs under big data conditions.

Deep Neural Network (DNN) Model

In the well grid optimization process, a Deep Neural Network (DNN) model is used for prediction to accurately estimate the key development parameters. The specific process structure is shown in Figure 8. First, eight parameters closely related to well grid optimization are selected for the input layer: average permeability, permeability variation, permeability rhythm, effective thickness of gas layers, gas layer thickness ratio, gas viscosity ratio, water multiple, and initial interlayer pressure difference. These parameters are represented as input vector $x = [x_1, x_2, \ldots, x_8]$, which are processed through weighted summation and activation functions at the first layer before being passed layer by layer to the hidden layers in the network.

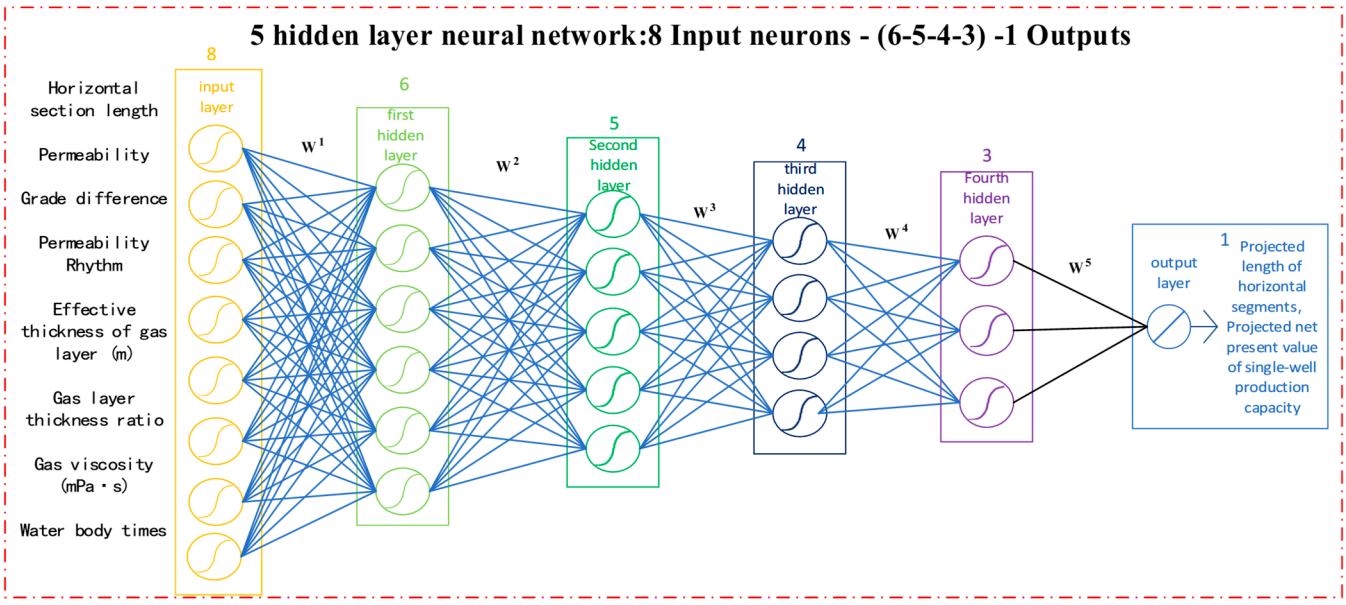


Figure 8. DNN model process flow diagram.

In the forward propagation of the DNN, the calculation at each layer is performed through weighted summation, $W^{(l)}a^{(l-1)} + b^{(l)}$, followed by a nonlinear activation function that introduces a nonlinear mapping, further extracting deeper feature information. This process continues until the fourth hidden layer, ensuring that the network learns the complex nonlinear relationships between the input parameters. After processing through the

four hidden layers, the output layer of the network generates two prediction results: horizontal segment length and the financial net present value of a single well. These two output parameters are the core indicators for well grid optimization, representing the optimal horizontal segment length and the economic benefit per well in the development process.

Through forward propagation, the model can obtain predicted values. To measure the difference between the predicted values and the true values, the loss function is constructed with w and b as variables. In this study, L2 regularization is selected as the loss function for the model.

$$loss(w, \lambda) = MSE + \lambda \times \sum_{i=1}^{l} w_i^{\ 2} \tag{2}$$

$$MSE = \frac{\sum_{i=1}^{n} (z_n - \hat{z}_n)^2}{n} \tag{3}$$

In this context, MES represents the variance function; λ is the regularization coefficient; and Zn denotes the true values. Subsequently, the backpropagation algorithm is employed to train and optimize the neural network. The core idea of backpropagation is to compute the gradients of the loss function with respect to the network parameters (weights and biases) for each layer using the chain rule, allowing adjustments to these parameters. During the training process, through multiple iterations, the network is continuously updated until the model's error reaches the desired range, and the training process converges. At this point, the DNN model has effectively learned the complex relationship between input parameters and output results through the backpropagation algorithm, enabling accurate predictions for new input data and achieving the goal of well pattern optimization.

The error gradient formula is as follows:

$$\delta_L = \frac{\partial L}{\partial a_L} \times f\prime(z_L) \tag{4}$$

Here, δ_i represents the error of the i-th layer, and W_{i+1} is the weight matrix of the i + 1-th layer.

$$W_i := W_i - \eta \times \frac{\partial L}{\partial W_i} \tag{5}$$

$$b_i := b_i - \eta \times \frac{\partial L}{\partial b_i} \tag{6}$$

Here, η is the learning rate, $\eta = 1 \times 10^{-4}$, $\frac{\partial L}{\partial W_i}$ and $\frac{\partial L}{\partial b_i}$ are the gradients of the weights and biases, respectively.

The specific code for the neural network can be found in Appendix A.

4. Result and Discussion

4.1. Verification Accuracy

Through training with 50 sets of simulated results, we found that due to the small size of the dataset, the model's prediction accuracy was relatively low. When the dataset was expanded to 150 sets, the prediction error for the single well net present value (NPV) decreased to 7.6%, and the error for horizontal section length decreased to 7.85%. These results indicate that as the dataset size increased, the prediction accuracy of the model improved significantly. It is important to note that the data we used were generated based on numerical simulations, derived from actual production data. However, since the study area is only a small experimental section of the gas field, we optimized the well pattern based on the actual drilling production data, made predictions using simulated data, and adjusted the well pattern parameters using history matching technology. The goal is to

optimize the well layout for future development. Our approach primarily aims to provide well pattern optimization recommendations for future development stages, rather than optimizing existing well data.

By utilizing actual production data, the combination of simulated data and history matching can effectively guide well pattern optimization, improving the model's prediction accuracy by adjusting parameters within the simulated data. In the future, we plan to conduct verification during actual production to further enhance the reliability and applicability of the model.

As shown in Figure 9, after the training dataset was increased from 50 sets to 150 sets, the error in the predicted horizontal section length decreased from 33.10% to 7.85%.

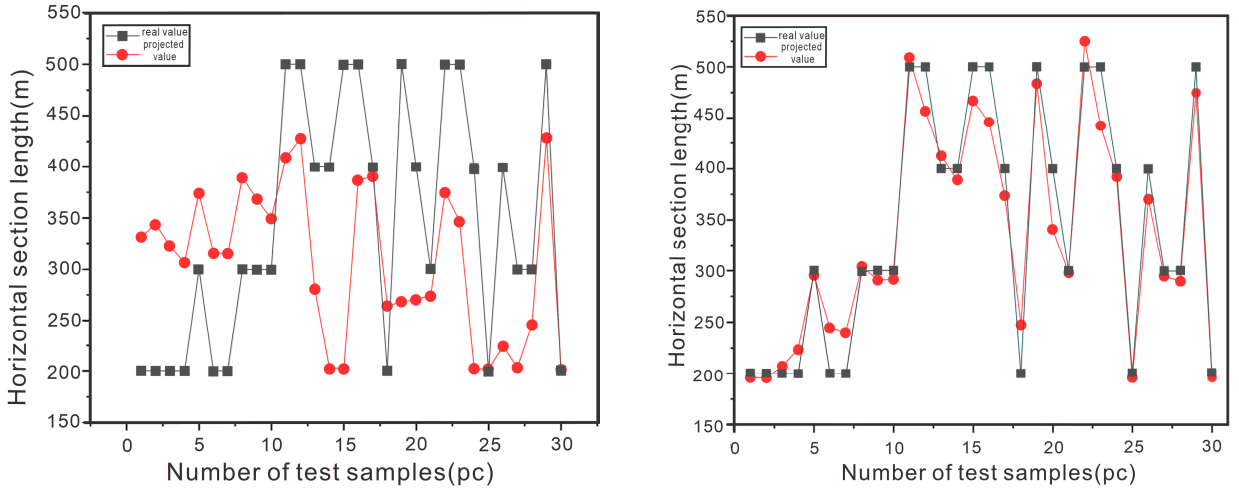


Figure 9. (**a**) Comparison of DNN model results with numerical model when the training set consists of 50 samples. (**b**) Comparison of DNN model results with numerical model results when the training set consists of 150 samples (horizontal section length prediction).

As shown in Figure 10, after the training dataset was increased from 50 sets to 150 sets, the error in the predicted single well productivity net present value decreased from 21.0% to 7.60%.

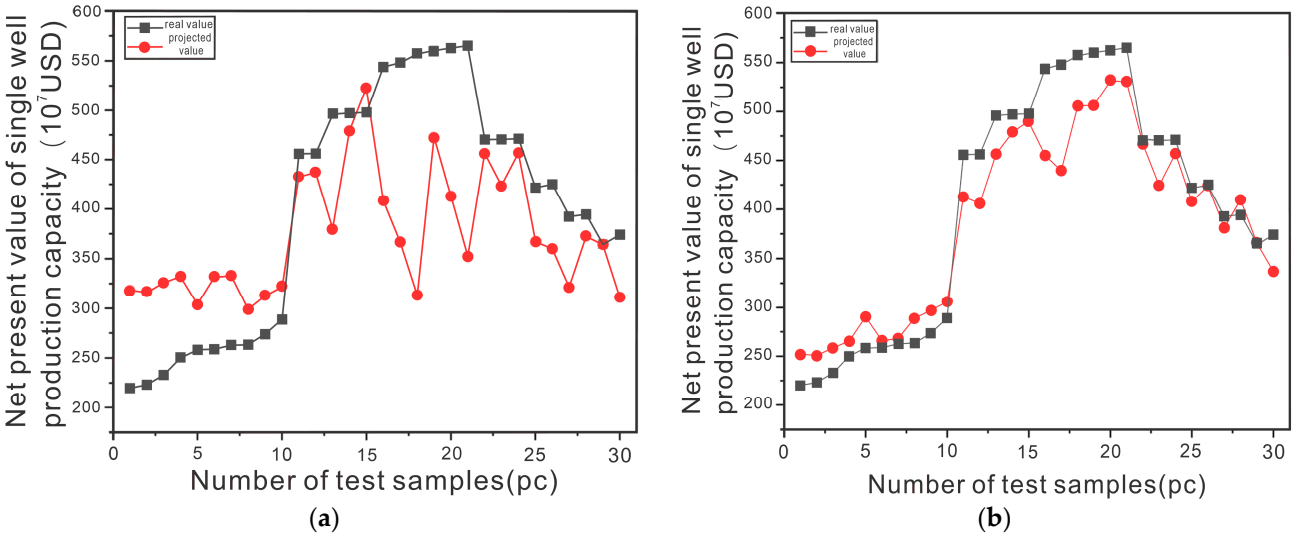


Figure 10. (**a**) Comparison of DNN model results with numerical model when the training set consists of 50 samples. (**b**) Comparison of DNN model results with numerical model results when the training set consists of 150 samples (single well productivity net present value prediction).

4.2. Appreciation

As shown in Figure 11, the well pattern optimization results show that the optimal segment lengths for step-type horizontal wells exhibit significant regional differences, which can be categorized into three main types: 1:2:1, 2:1:1, and 1:1:2. The distribution of these optimal ratios is closely related to the physical properties of the reservoir, especially the variations in factors such as the water drive multiple, gas viscosity ratio of each sublayer, permeability range, and permeability rhythm, all of which have a significant impact on the optimization of the horizontal segment length ratio.

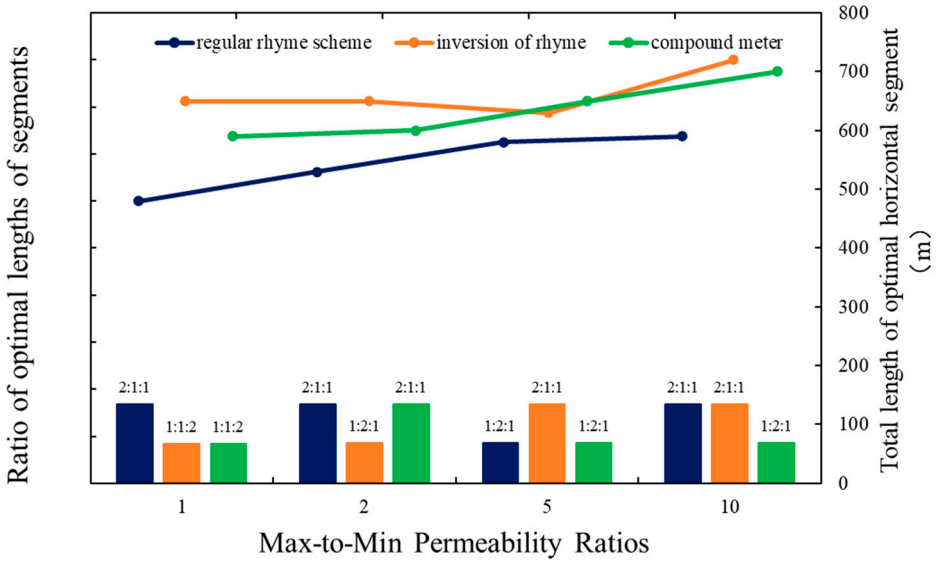


Figure 11. Optimal horizontal segment length and length ratios under different permeability rhythm and permeability range conditions.

As shown in Figure 12, under different water drive multiples, the well pattern optimization results indicate that when the water drive multiple is high, the gas production is more affected by water invasion. Therefore, a layout with longer front segments and shorter rear segments (i.e., 1:2:1 ratio) is preferred. This layout helps to better develop the main gas source regions in the gas reservoir and reduce the productivity loss caused by water invasion. In contrast, when the water drive multiple is low, the optimization results tend to favor a more uniform length ratio (such as 2:1:1 or 1:1:2) to achieve balanced productivity across the segments and avoid overdevelopment of the front segment.

The gas viscosity ratio of each sublayer is also an important factor influencing the horizontal segment length ratio. For layers with higher gas viscosity, the optimization results show that the optimal horizontal segment length is shorter to reduce flow resistance and improve gas flow efficiency. Under conditions of lower gas viscosity, the optimization results tend to favor longer front or middle segments to fully develop the gas reservoir's productivity and increase overall production.

Furthermore, variations in permeability range and permeability rhythm also influence the choice of optimal length ratios. When the permeability range is large, indicating significant reservoir heterogeneity, the optimization results tend to adopt a 1:2:1 or 2:1:1 layout, which helps to concentrate gas development in lower permeability layers while maintaining shorter horizontal segment lengths in higher permeability areas. In regions with better permeability rhythm, a 1:1:2 ratio layout is typically used to achieve uniform gas development across layers.

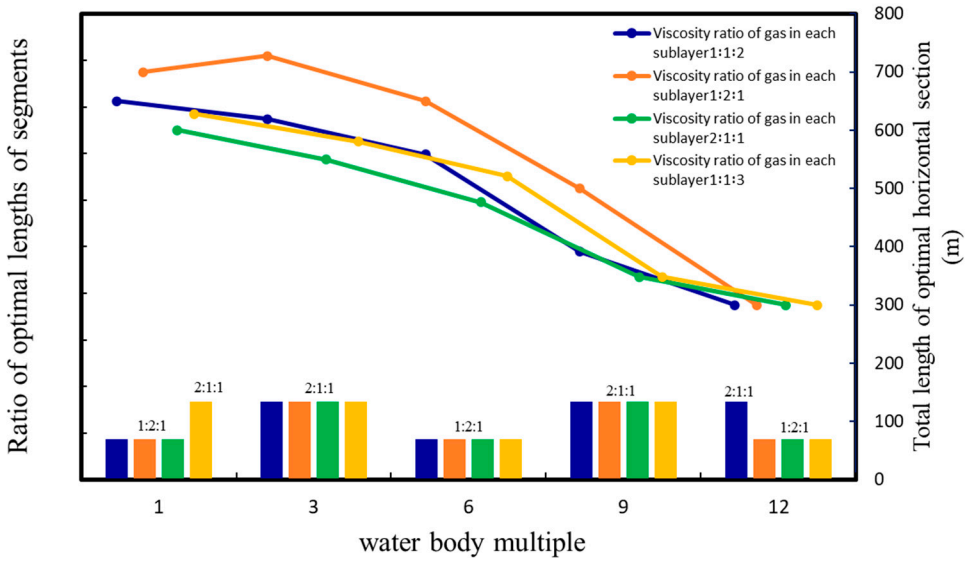


Figure 12. Optimal horizontal segment length and length ratios under different water drive multiples and gas viscosity ratios of each sublayer.

4.3. Superiority

This paper optimizes the well pattern parameters of the gas reservoir in the study area by combining fine numerical simulation with Deep Neural Network (DNN) technology. The study focuses on analyzing the impact of horizontal well section length and length ratios on reservoir productivity, and a refined well pattern optimization model was developed. Based on this, we proposed an optimization strategy for the stepped horizontal well length and segment length ratios. This method has improved the efficiency of well pattern optimization to some extent. Compared to traditional numerical simulation methods, it reduces the workload of manually adjusting parameters and offers a more automated optimization solution. However, it is worth noting that this method is currently mainly applicable to well pattern optimization in multilayer thin gas reservoirs, and further validation and adjustments may be required for other types of reservoirs. We believe that with the support of more actual data, the adaptability and application range of the method are expected to be further extended.

5. Conclusions

1. This study proposes a comprehensive well pattern optimization method, combining three-dimensional geological modeling, numerical simulation technology, orthogonal experimental analysis, and Deep Neural Network (DNN) models. This approach represents an innovative effort to address well pattern optimization for multilayered thin gas reservoirs.
2. By analyzing the degree of extraction and gas production changes per unit footage for different well types, as well as the 15-year financial net present value changes for various well types, the step-type horizontal well has been identified as a potentially optimal well type for the research area, based on the available data.
3. Using orthogonal experimental methods, the well pattern parameters for the study area have been optimized as follows: a well spacing of 2500 m, 5 wells, a horizontal segment ratio of 1:2:1, and a well pattern direction of N-W 80°. These parameters offer a promising starting point for future field application, but further verification is needed.
4. Through the orthogonal experiment, 8 relevant parameters were selected, and 150 experimental schemes were designed. By integrating the Deep Neural Network, a well

pattern optimization model was constructed, yielding an error of 7.6% for the single well productivity net present value and 7.85% for the horizontal segment length. These results suggest that the proposed model has the potential for well pattern optimization in multilayered thin gas reservoirs, though further testing and validation in diverse reservoir conditions are necessary to confirm its effectiveness and applicability.

5. Although the well network optimization method based on the DNN algorithm proposed in this paper has achieved good results in multilayer thin gas reservoirs, its applicability is somewhat limited. Specifically, the proposed method currently focuses primarily on the well network optimization of multilayer thin gas reservoirs, which are characterized by specific geological features. For other types of gas reservoirs, such as thick gas reservoirs, heterogeneous gas reservoirs, or those with complex geological conditions, further adjustments and optimizations may be required. More field validation and adaptability testing are needed to confirm its feasibility and effectiveness in different types of gas reservoirs.

Author Contributions: C.T.: Visualization; investigation; methodology; writing—original draft. Y.C.: Data curation; writing—original draft. X.L.: Supervision. C.T. and L.L.: Resources; conceptualization. Y.C. and L.Q.: Writing—review and editing. All authors have read and agreed to the published version of the manuscript.

Funding: This research was funded by the CNPC Innovation Fund (2022DQ02-0202).

Data Availability Statement: The datasets generated and/or analyzed during the current study are available from the corresponding author on reasonable request.

Conflicts of Interest: All authors of the manuscript affirm that the research was conducted without any potential conflicts of interest arising from commercial or financial relationships.

Appendix A

The code for the Deep Neural Network in the paper can be found at the following website: https://github.com/liang2517/Well-pattern-optimization-for-multilayer-thin-gas-reservoirs (accessed on 17 February 2025).

References

1. Cheng, Y.Y.; Mu, L.X.; Zhu, E.Y.; Zhang, P.J.; Guo, C.Q.; Leng, Y.H.; Wei, Z.J.; Chen, P.Y.; Xing, Y.Z.; Cheng, M.W.; et al. Water producing mechanisms of carbonate reservoirs gas wells: A case study of the Right Bank Field of Amu Darya, Turkmenistan. *Pet. Explor. Dev.* **2017**, *44*, 89–96. [CrossRef]
2. Lei, Q.; Yang, L.F.; Duan, Y.Y.; Weng, D.W.; Wang, X.; Guan, B.S.; Wang, Z.; Guo, Y. The "fracture-controlled reserves" based stimulation technology for unconventional oil and gas reservoirs. *Pet. Explor. Dev.* **2018**, *45*, 770–778. [CrossRef]
3. Ma, X.H. "Extreme utilization" development theory of unconventional natural gas. *Pet. Explor. Dev.* **2021**, *48*, 381–394. [CrossRef]
4. Wei, S.; Qiu, K.X. Pressure Analysis of Onshore and Offshore Shale Gas Reservoirs under Constant-Rate Condition Considering Thin Sandstone Layer and Interlayer Cross-Flow. *J. Mar. Sci. Eng.* **2024**, *12*, 457. [CrossRef]
5. Bian, X.B.; Zhang, S.C.; Zhang, J.C.; Wang, D.B. Well spacing design for low and ultra-low permeability reservoirs developed by hydraulic fracturing. *Pet. Explor. Dev.* **2015**, *42*, 705–711. [CrossRef]
6. He, D.B.; Wang, L.J.; Ji, G.; Wei, Y.S.; Jia, C.Y. Well spacing optimization for Sulige tight sand gas field, NW China. *Pet. Explor. Dev.* **2012**, *39*, 491–497. [CrossRef]
7. Li, G.X.; Qin, J.H.; Xian, C.G.; Fan, X.B.; Zhang, J.; Ding, Y. Theoretical understandings, key technologies and practices of tight conglomerate oilfield efficient development: A case study of the Mahu oilfield, Junggar Basin, NW China. *Pet. Explor. Dev.* **2020**, *47*, 1275–1290. [CrossRef]
8. He, D.B.; Jia, A.L.; Ji, G.; Wei, Y.S.; Tang, H.F. Well type and pattern optimization technology for large scale tight sand gas, Sulige gas field, NW China. *Pet. Explor. Dev.* **2013**, *40*, 84–95. [CrossRef]
9. He, J.; Li, A.W.; Wu, S.S.; Tang, R.X.; Lv, D.L.; Li, Y.R.; Li, X.B. Experimental Investigation on Injection and Production Pattern in Fractured-Vuggy Carbonate Reservoirs. *Energies* **2020**, *13*, 603. [CrossRef]

10. Liu, J.; Liu, Y.T.; Zhang, J.C.; Yang, J.; Guo, Z.L. Experimental and Simulation Study of Complex Structure Well Pattern Optimization for Buried Hill Fractured Reservoirs. *Arab. J. Sci. Eng.* **2014**, *39*, 8347–8358. [CrossRef]
11. Jang, I.; Oh, S.; Kim, Y.; Park, C.; Kang, H. Well-placement optimisation using sequential artificial neural networks. *Energy Explor. Exploit.* **2018**, *36*, 433–449. [CrossRef]
12. Mousavi, S.H.R.; Hosseini-Nasab, S.M. Residual Convolutional Neural Network for Lithology Classification: A Case Study of an Iranian Gas Field. *Int. J. Energy Res.* **2024**, *2024*, 5576859. [CrossRef]
13. Mousavi, S.H.R.; Hosseini-Nasab, S.M. A novel approach to classify lithology of reservoir formations using GrowNet and Deep-Insight with physic-based feature augmentation. *Energy Sci. Eng.* **2024**, *12*, 4453–4477. [CrossRef]
14. Gao, D.P.; Ye, J.G.; Wang, T.J.; Liang, Z.; Pan, S.Q.; Sun, Z.L. An independent fracturing water-flooding development method for shallow low-permeability thin oil layers in multi-layer sandstone reservoirs. *J. Pet. Sci. Eng.* **2018**, *167*, 877–889.
15. Liu, Y.C.; Luo, X.B.; Kang, K.; Li, T.L.; Jiang, S.H.; Zhang, J.; Zhang, Z.; Li, Y.T. Permeability characterization and directional wells initial productivity prediction in the continental multilayer sandstone reservoirs: A case from Penglai 19-3 oil field, Bohai Bay Basin. *Pet. Explor. Dev.* **2017**, *44*, 97–104. [CrossRef]
16. Hu, W.R.; Wei, Y.; Bao, J.W. Development of the theory and technology for low permeability reservoirs in China. *Pet. Explor. Dev.* **2018**, *45*, 685–697. [CrossRef]
17. Qun, L.; Yun, X.; Bo, C.; Baoshan, G.; Xin, W.; Guoqiang, B.; Hui, L.; Shuai, L.; Bin, D.; Haifeng, F.; et al. Progress and prospects of horizontal well fracturing technology for shale oil and gas reservoirs. *Pet. Explor. Dev.* **2022**, *49*, 191–199.
18. Cheng, Y.Y.; Luo, X.; Lu, T.Y.; Guo, C.Q.; Tan, C.Q. Well-Controlled Dynamic Reserves Calculation of Abnormally High-Pressured Gas Reservoirs Developed with Edge and Bottom Aquifers. *Processes* **2023**, *11*, 938. [CrossRef]
19. Deng, C.H. Vector well pattern optimization of horizontal well in offshore edge water reservoirs. *Front. Energy Res.* **2023**, *11*, 1226328. [CrossRef]
20. Feng, X.X.; Liao, X.W. Study on Well Spacing Optimization in a Tight Sandstone Gas Reservoir Based on Dynamic Analysis. *Acs Omega* **2020**, *5*, 3755–3762. [CrossRef]
21. Zoeir, A.; Riazi, M.; Kazemzadeh, Y.; Khodapanah, E. To optimize well pattern during miscible gas injection process via heuristic techniques. *J. Pet. Sci. Eng.* **2022**, *208*, 109786. [CrossRef]
22. Zheng, R.C.; Li, Y.; Wu, L.; Wu, X.Z.; Li, F.J.; Niu, G. Geochemical characteristics of Callovian-Oxfordian carbonates in Samandepe gas field, Amu Darya Basin, Turkmenistan. *Pet. Sci.* **2011**, *8*, 371–381. [CrossRef]
23. Liao, J.B.; Zhang, Z.Y.; Tang, H.Z.; Yang, J.; Zhang, X.L.; Wang, B. Simulation of Fracturing and Well Pattern Optimization of Fractured Tight Sandstone Reservoirs. *Front. Earth Sci.* **2022**, *10*, 873617. [CrossRef]
24. Yu, Y.X.; Yin, J.Y.; Zheng, J.Z.; Li, F.; Tao, C.Z.; Xu, X.L.; Wu, H. Division and resources evaluation of hydrocarbon plays in the Amu Darya basin, central Asia. *Pet. Explor. Dev.* **2015**, *42*, 819–826. [CrossRef]
25. Jiang, L.; Gao, P.; Liu, J.; Xiong, Y.B.; Jiang, J.; Jia, R.Z.; Li, Z.C.; Liu, P.C. Simulation and Optimization of Dynamic Fracture Parameters for an Inverted Square Nine-Spot Well Pattern in Tight Fractured Oil Reservoirs. *Geofluids* **2020**, *2020*, 8883803. [CrossRef]
26. Wang, B.; Zhao, Y.J.; Tian, Y.J.; Kong, C.L.; Ye, Q.Y.; Zhao, S.C.; Li, Z.H.; Suo, Y. Numerical Simulation Study of Pressure-Driven Water Injection and Optimization Development Schemes for Low-Permeability Reservoirs in the G Block of Daqing Oilfield. *Processes* **2024**, *12*, 1. [CrossRef]
27. Ren, L.; Wang, J.Z.; Zhao, C.; Jing, C.; Sun, J.; Zhou, D.S.; Xiang, F.G.; Gong, D.G.; Li, H.Y. Optimization of Fine-Fracture Distribution Patterns for Multi-Stage and Multi-Cluster Fractured Horizontal Wells in Tight Gas Reservoirs. *Processes* **2024**, *12*, 1392. [CrossRef]
28. Sun, L.; Li, B.Z.; Li, Y. Productivity Models of Infill Complex Structural Wells in Mixed Well Patterns. *Processes* **2019**, *7*, 324. [CrossRef]
29. Tian, H.; Liao, K.; Liu, J.K.; Chen, Y.C.; Ma, J.; Wang, Y.P.; Song, M.R. Flowback Characteristics Analysis and Rational Strategy Optimization for Tight Oil Fractured Horizontal Well Pattern in Mahu Sag. *Processes* **2023**, *11*, 3377. [CrossRef]
30. Zhao, C.S.; Li, P.J.; Guan, D.; Liu, Q.J. Optimization of horizontal well staggered patterns. *Pet. Sci.* **2008**, *5*, 348–352. [CrossRef]
31. Wang, D.Y.; Fang, M.J.; Li, H.; Cao, G.S.; Fan, W.P.; Wang, B. A New Method for Determining Economic Well Pattern Density and Infilling Time of Tight Gas Reservoirs. *Energies* **2024**, *17*, 1223. [CrossRef]
32. Wang, H.; Chen, Z.; Chen, S.N.; Hui, G.; Kong, B. Production forecast and optimization for parent-child well pattern in unconventional reservoirs. *J. Pet. Sci. Eng.* **2021**, *203*, 108899. [CrossRef]
33. Wang, X.; Haynes, R.D.; Feng, Q.H. A multilevel coordinate search algorithm for well placement, control and joint optimization. *Comput. Chem. Eng.* **2016**, *95*, 75–96. [CrossRef]
34. Yin, R.W.; Li, Q.Y.; Li, P.C.; Lu, D.T. Parameter Identification of Multistage Fracturing Horizontal Well Based on PSO-RBF Neural Network. *Sci. Program.* **2020**, *2020*, 6810903. [CrossRef]
35. Yin, X.J.; Lu, S.Y.; Wang, Y.X.; Du, Z.L.; Li, Y.X. Optimization study of encrypted deployment for dense well network. *Energy Rep.* **2022**, *8*, 756–762. [CrossRef]

36. Zhan, J.; Tian, Y.F.; Fan, C.; Ma, X.L.; Nie, R.S.; Ji, D.Q.; Li, T.; Yu, H.Y. Well Pattern and Well Spacing Optimization of Large Volume Water Injection in a Low-Permeability Reservoir with Pressure Sensitivity. *Geofluids* **2022**, *2022*, 8215223. [CrossRef]
37. Lye, K.O.; Mishra, S.; Ray, D.; Chandrashekar, P. Iterative surrogate model optimization (ISMO): An active learning algorithm for PDE constrained optimization with deep neural networks. *Comput. Methods Appl. Mech. Eng.* **2021**, *374*, 113575. [CrossRef]
38. Tang, L.H.; Li, J.J.; Lu, W.M.; Lian, P.Q.; Wang, H.; Jiang, H.Q.; Wang, F.L.; Jia, H.G. Well Control Optimization of Waterflooding Oilfield Based on Deep Neural Network. *Geofluids* **2021**, *2021*, 8873782. [CrossRef]
39. Zaheri, S.H.; Hosseini, M.; Fathinasab, M. Well Pattern optimization as a planning process using a novel developed optimization algorithm. *Sci. Rep.* **2024**, *14*, 26725. [CrossRef]
40. Zhang, K.; Chen, Y.X.; Zhang, L.M.; Yao, J.; Ni, W.; Wu, H.Y.; Zhao, H.; Lee, J.I. Well pattern optimization using NEWUOA algorithm. *J. Pet. Sci. Eng.* **2015**, *134*, 257–272. [CrossRef]

Disclaimer/Publisher's Note: The statements, opinions and data contained in all publications are solely those of the individual author(s) and contributor(s) and not of MDPI and/or the editor(s). MDPI and/or the editor(s) disclaim responsibility for any injury to people or property resulting from any ideas, methods, instructions or products referred to in the content.